

Supplementary Materials for

Scalable-Produced 3D Elastic Thermoelectric Network for Body Heat Harvesting

Yijie Liu^{a, b, #}, Xiaodong Wang^{c, #}, Shuaihang Hou^c, Zuoxu Wu^b, Jian Wang^b, Jun Mao^{c, d}, Qian Zhang^{c, d, *}, Zhiguo Liu^{a, *}, Feng Cao^{b, *}

^a School of Physics, Harbin Institute of Technology, Harbin 150001, P. R. China
liuzhiguo@hit.edu.cn

^b School of Science, and Ministry of Industry and Information Technology Key Lab of Micro-Nano Optoelectronic Information System, Harbin Institute of Technology, Shenzhen 518055, P. R. China caofeng@hit.edu.cn

^c School of Materials Science and Engineering, Institute of Materials Genome & Big Data, and Flexible Printed Electronics Technology Center, Harbin Institute of Technology, Shenzhen 518055, P. R. China zhangqf@hit.edu.cn

^d State Key Laboratory of Advanced Welding and Joining, Harbin Institute of Technology, Harbin 150001, P. R. China

Equal contribution

Inventory of Supplementary Information:

- Supplementary Figures S1-S19 Page 2-20
- Supplementary Tables S1-S2 Page 21
- Supplementary References 1-4 Page 22

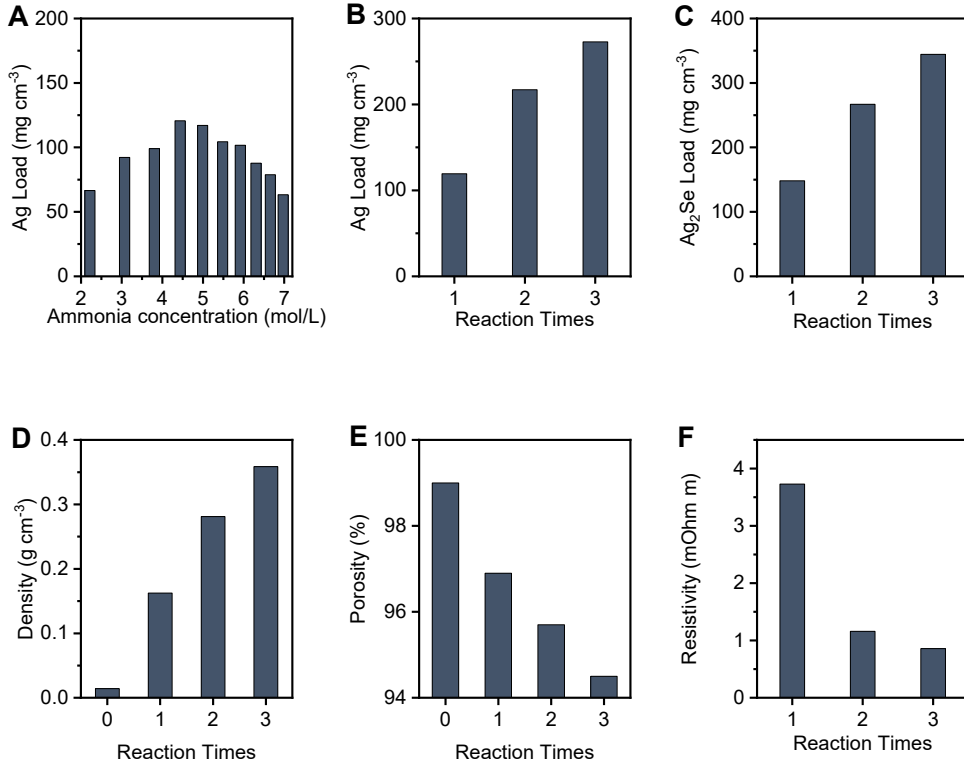


Fig. S1. **A**, The silver load with different ammonia concentration. The ammonia concentration with maximum loads was adopted for subsequent experiments. **B**, The silver load with different silvering times. **C**, The silver selenide load with different silvering times. **D**, The density of Ag₂Se network with different silvering times. The number of 0 represents the pristine melamine template before reaction. **E**, Porosity of the Ag₂Se networks were tested by the Archimedes method. **F**, Resistivity of the Ag₂Se network with different loads.

The principle of the Archimedes method is given as follows:

The weights of the dry sample in air (m_1), the sample fully filled with alcohol both in air (m_2) and in alcohol (m_3) were measured. Then the Ag₂Se network's volume V_{network} (excluding pores) can be calculated using

$$V_{\text{network}} = \frac{m_1 - m_3}{\rho_{\text{alcohol}}} \quad (1)$$

where ρ_{alcohol} is the density of alcohol. The pores' volume V_{pores} (excluding network) can be calculated using

$$V_{\text{pores}} = \frac{m_2 - m_1}{\rho_{\text{alcohol}}} \quad (2)$$

So, the porosity of the Ag₂Se network can be expressed as

$$\text{Porosity} = \frac{V_{\text{pores}}}{V_{\text{pores}} + V_{\text{network}}} = \frac{m_2 - m_1}{m_2 - m_3} \quad (3)$$

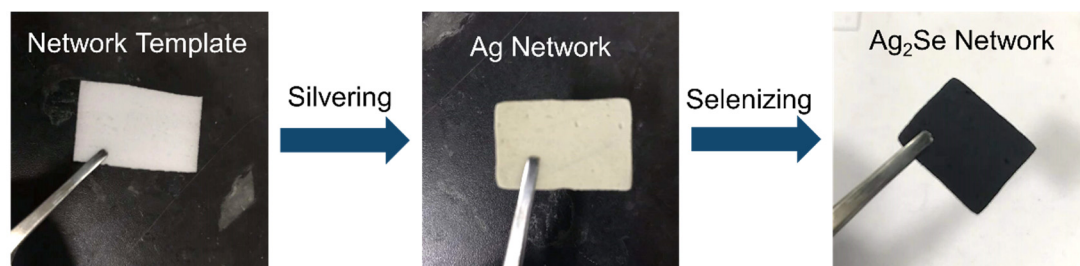


Fig. S2. The color changes in the reaction process.

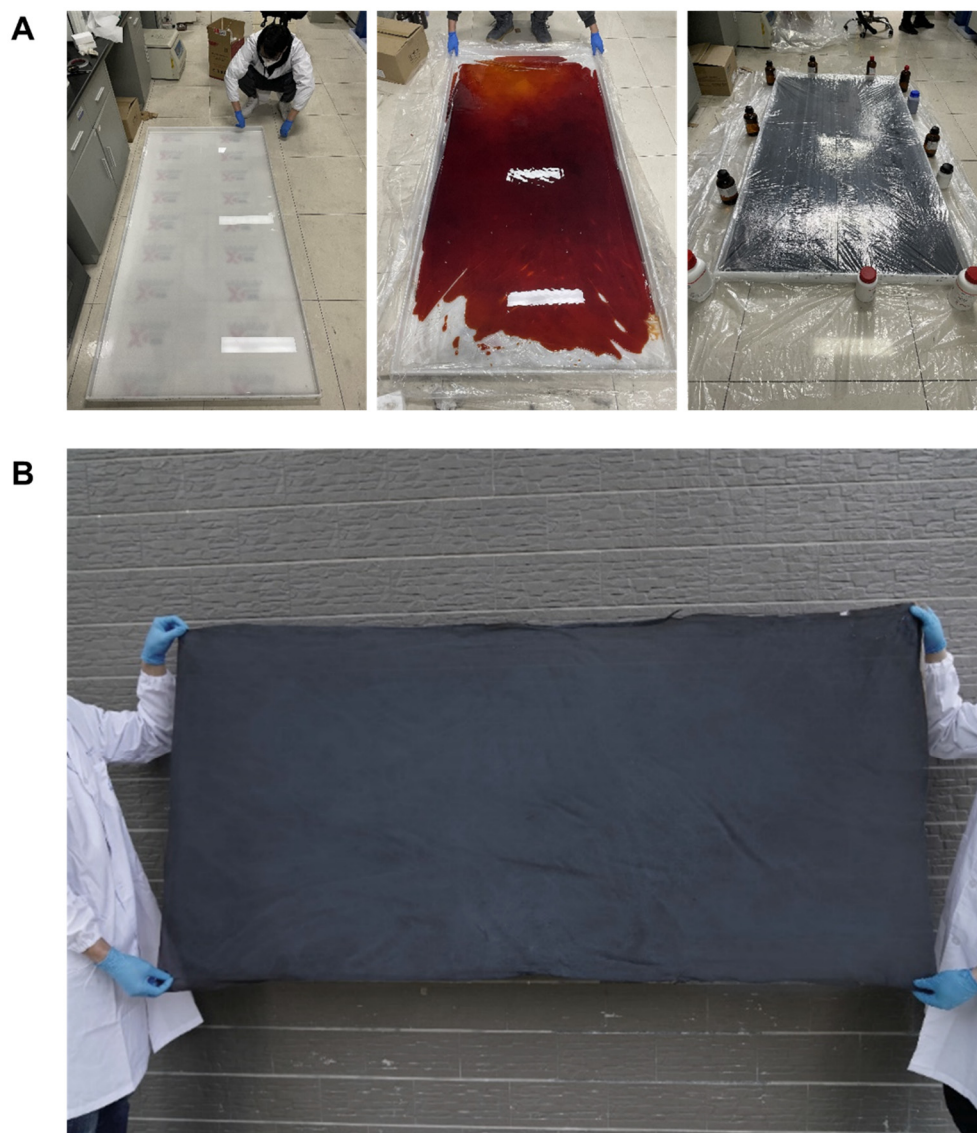


Fig. S3. **A**, The mass preparation process. **B**, The prepared large size Ag_2Se network.

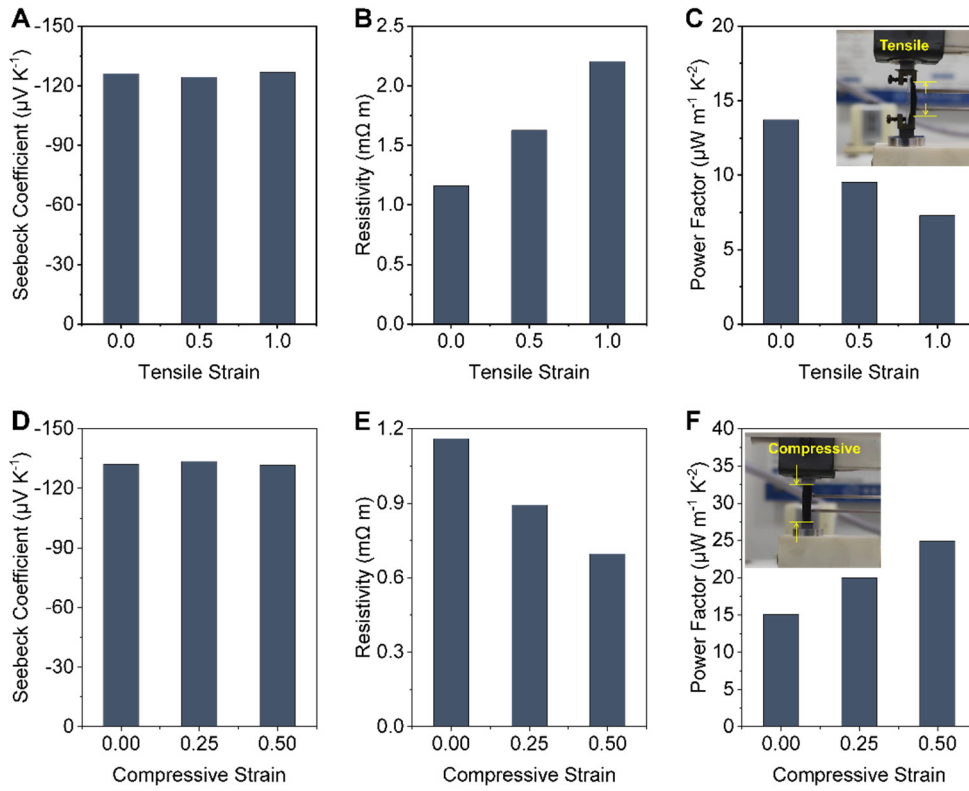


Fig. S4. The room-temperature Seebeck coefficient (A, D), resistivity (B, E) and power factor (C, F) of the Ag₂Se network under different strains.

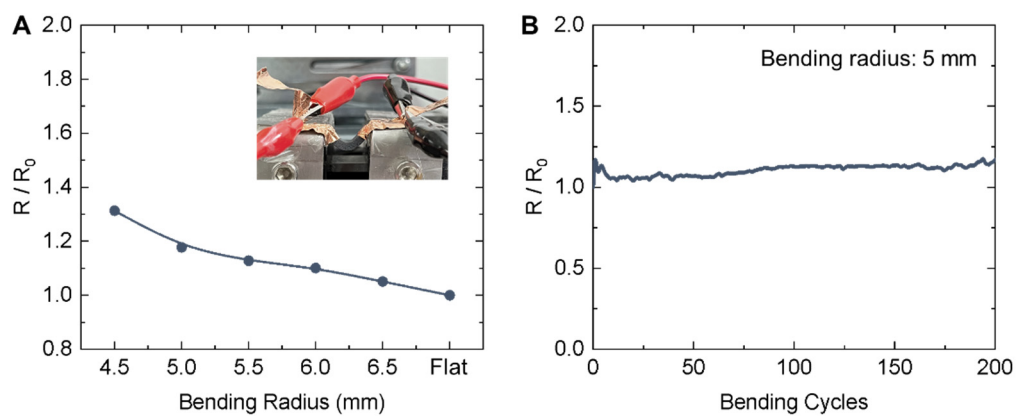


Fig. S5. **A**, Bending radius-dependent and **B**, bending cycles-dependent normalized resistance of the proposed Ag_2Se network.

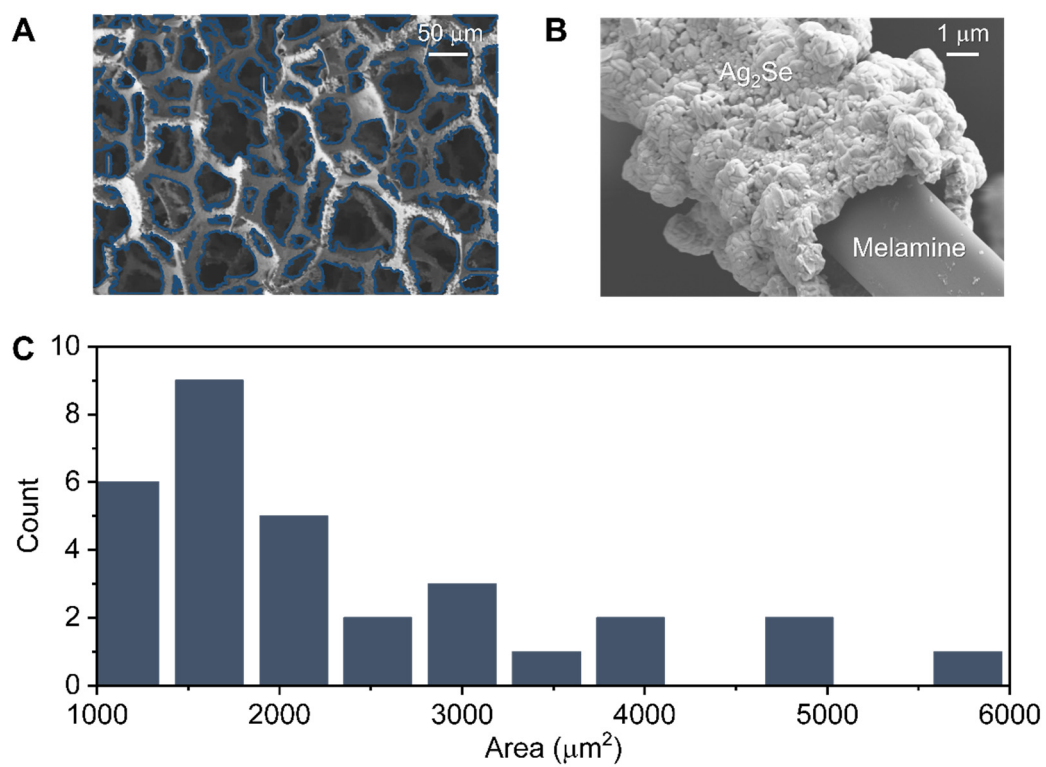


Fig. S6. **A**, The cross-section morphology of Ag₂Se network. **B**, A detailed image of Ag₂Se wrapping on a melamine fiber. **C**, Distribution of the pore size.

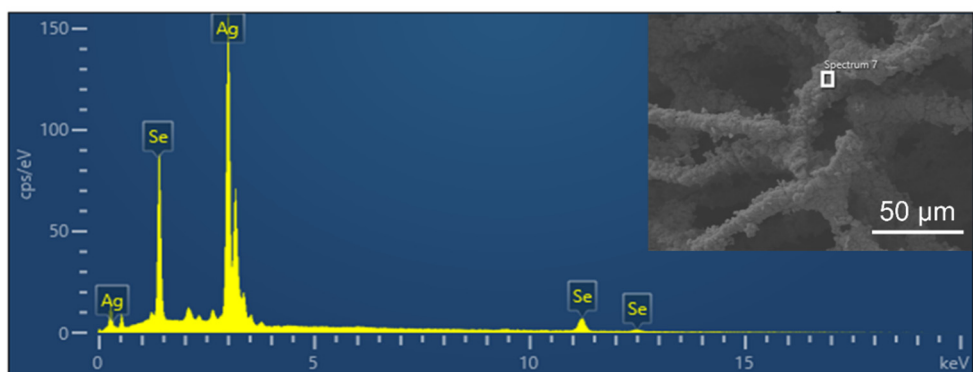


Fig. S7. Energy dispersive spectrum of Ag₂Se network.

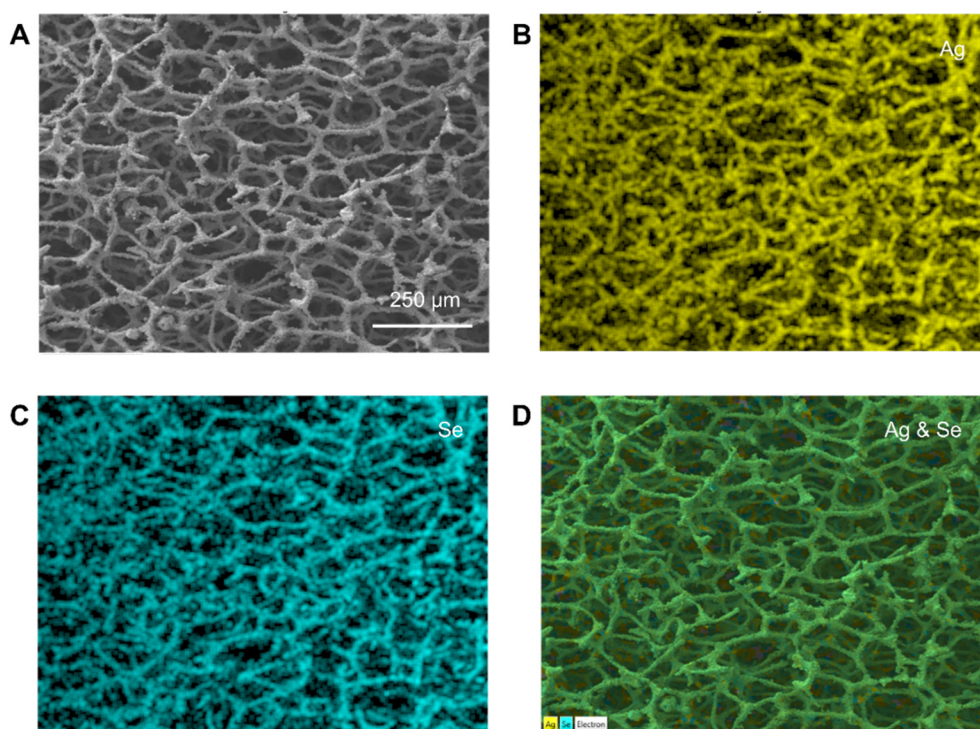


Fig. S8. The distribution of elements in Ag_2Se network.

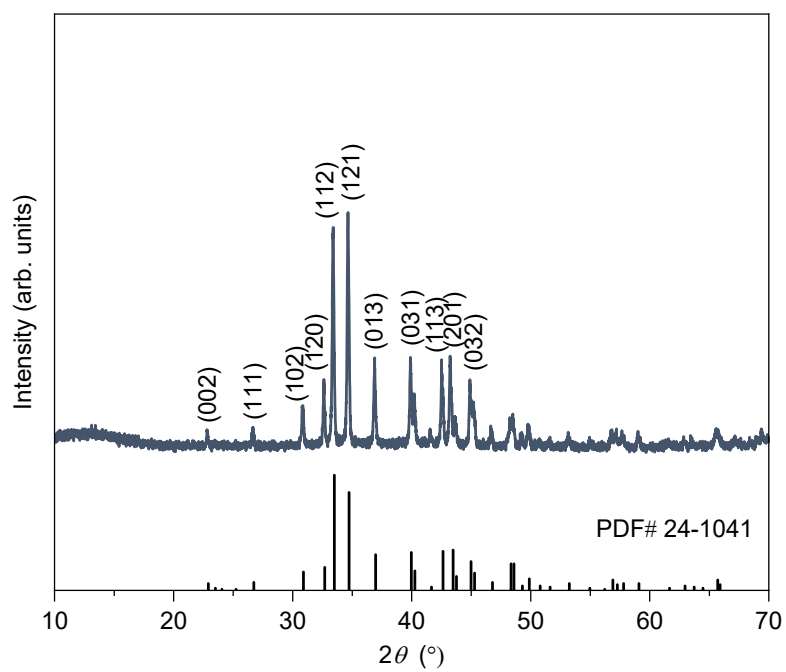


Fig. S9. XRD pattern of Ag₂Se network. The obtained Ag₂Se network is single phase without any impurities.

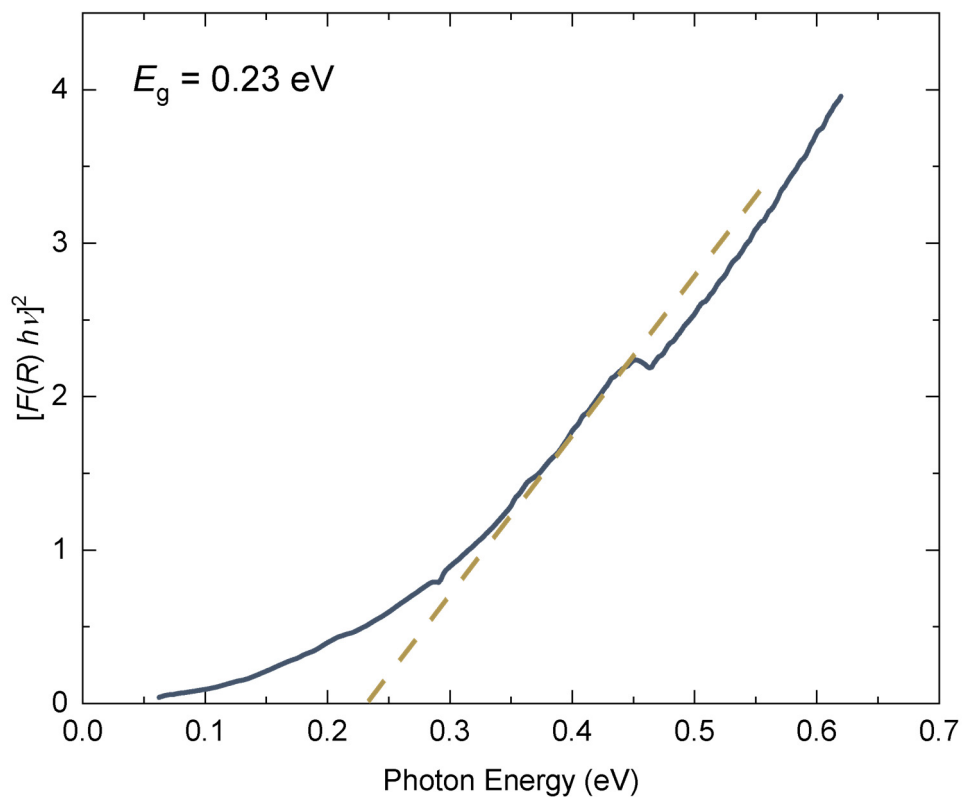


Fig. S10. Kubelka-Munk transformed reflectance spectra of Ag₂Se network.

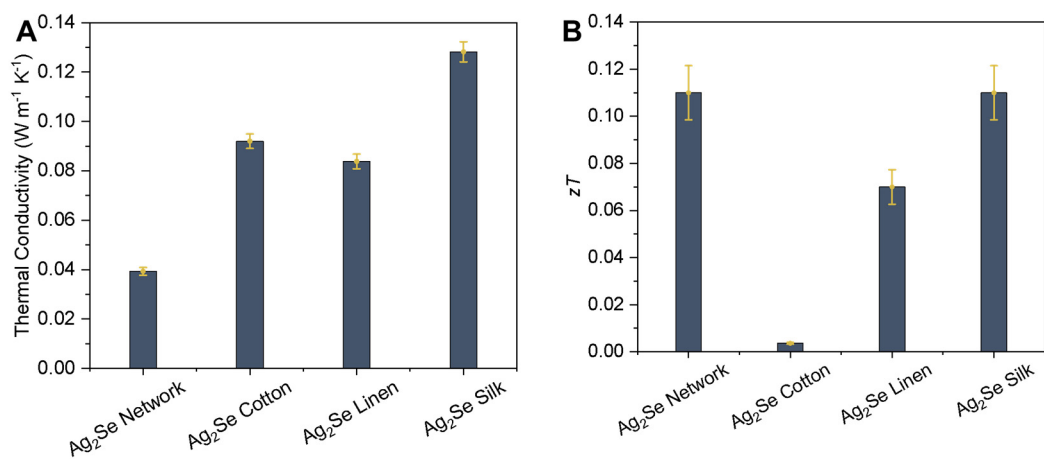


Fig. S11. A, Thermal conductivity and **B**, Room-temperature zT of the Ag₂Se network and Ag₂Se fabrics. Bars and error bars show the mean of the three readings and uncertainty of the results, respectively.

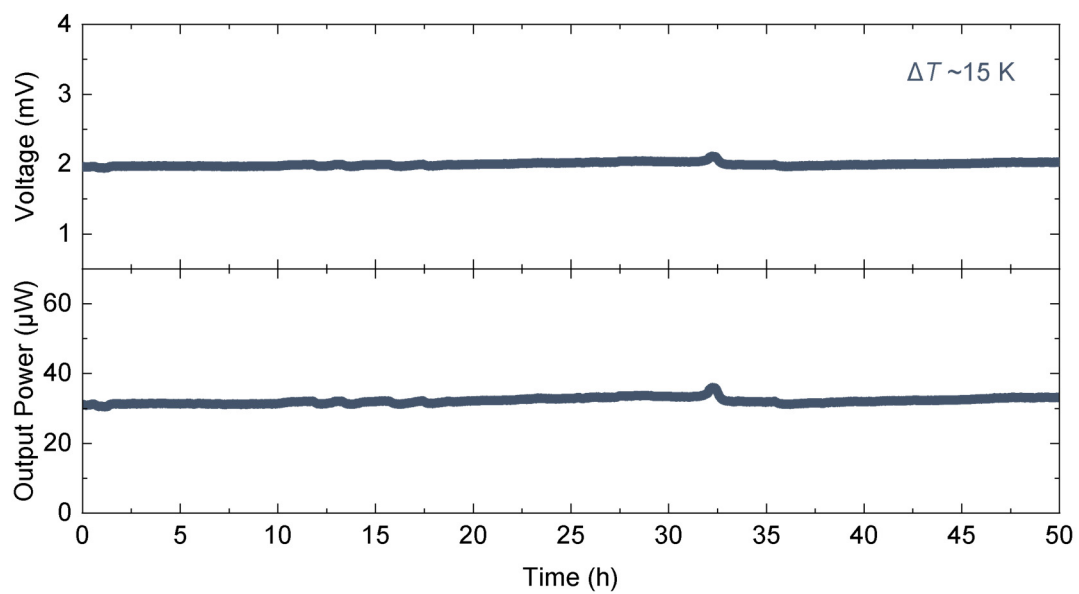


Fig. S12. The output performance changes with time at a fixed temperature difference of ~ 15 K.

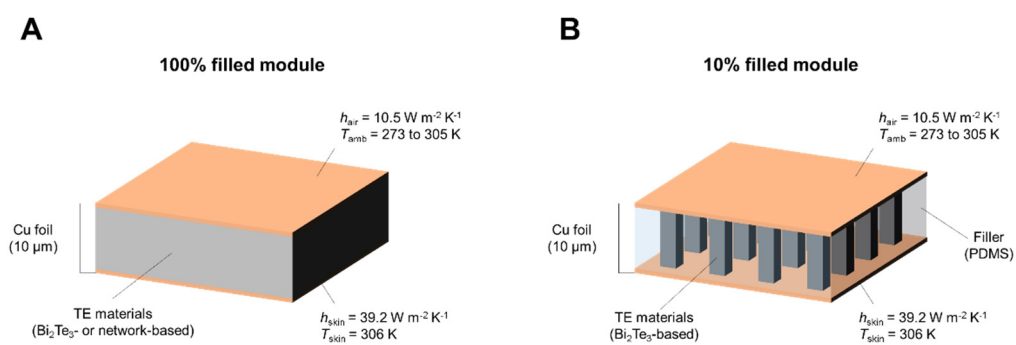


Fig. S13. Schematics of the simulation models. **A**, The Bi_2Te_3 -based or Ag_2Se network based module with a fill factor of 100%. **B**, The Bi_2Te_3 -based module with a fill factor of 10%. The specific material properties and the parameters' source were provided in Table S2.

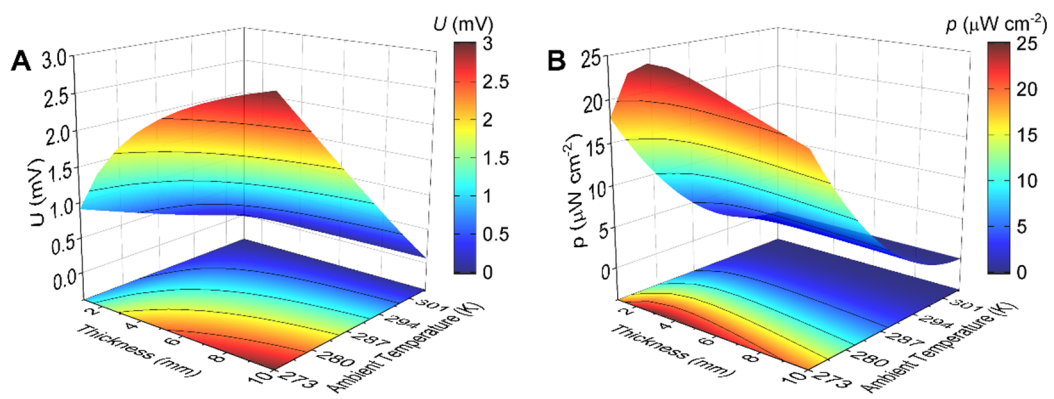


Fig. S14. **A**, Open-circuit voltage (U) and **B**, power density (p) of the network-based FTEG with different module thickness and ambient temperature.



Fig. S15. **A**, Thermolectric jacket. **B**, The padded network-based FTEG.

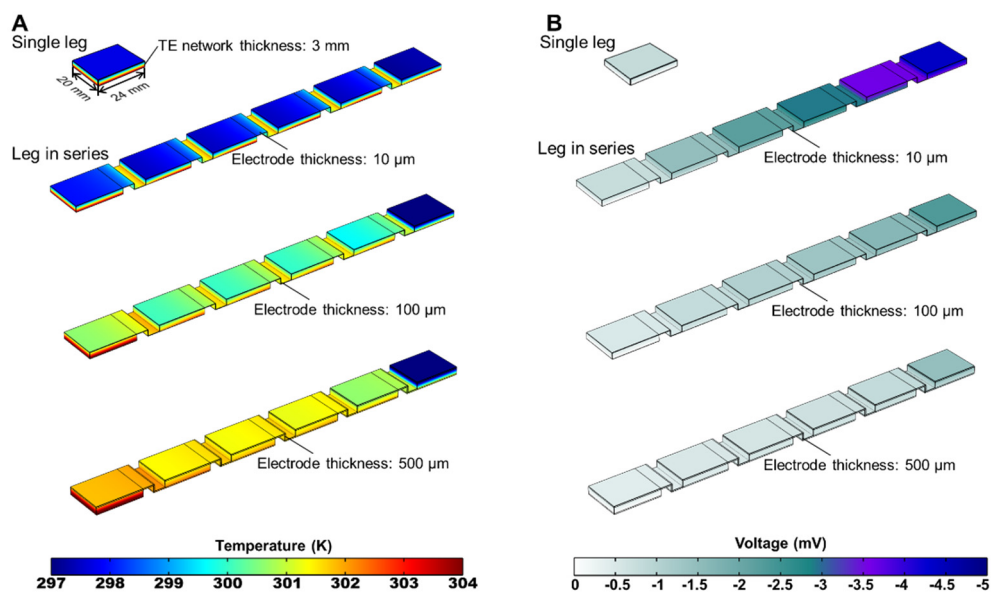


Fig. S16. Temperature distribution (**A**) and potential distribution (**B**) of the single leg and 6 legs in series. To further explain the effect of electrode thickness on temperature difference, we simulated the device with the same situation but thicker electrodes (eg., 100 μm and 500 μm). The device with thicker electrodes is difficult to establish temperature and potential differences.

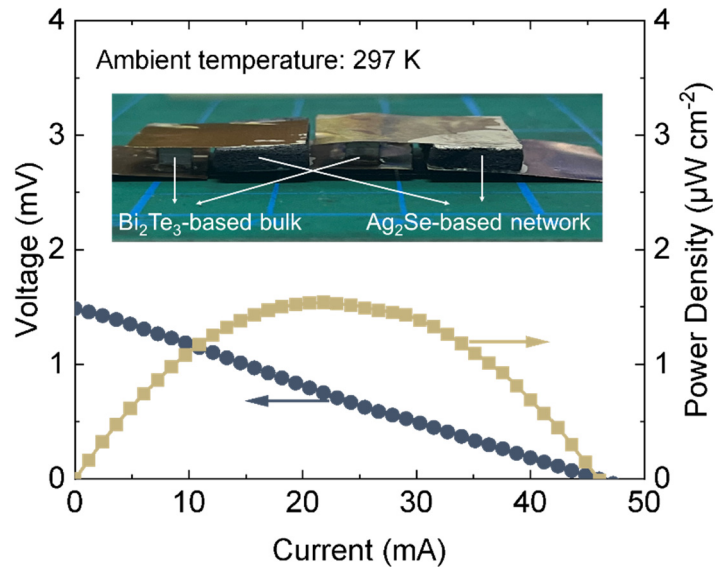


Fig. S17. Output performance of the FTEG with p-type Bi₂Te₃-based bulks and n-type Ag₂Se-based networks.

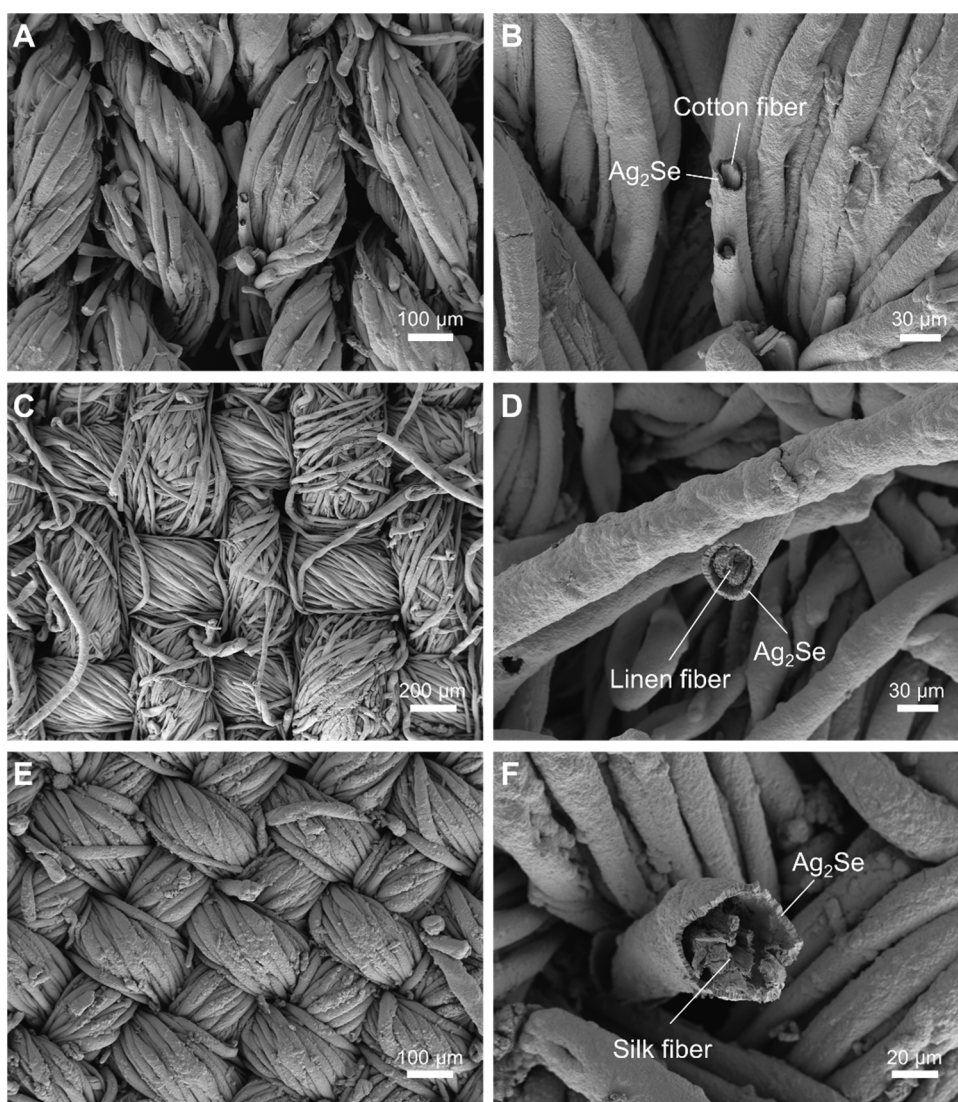


Fig. S18. The micrographs of various thermoelectric fabrics. **A** and **B**, Cotton fabrics. **C** and **D**, Linen fabrics. **E** and **F**, Silk fabrics.

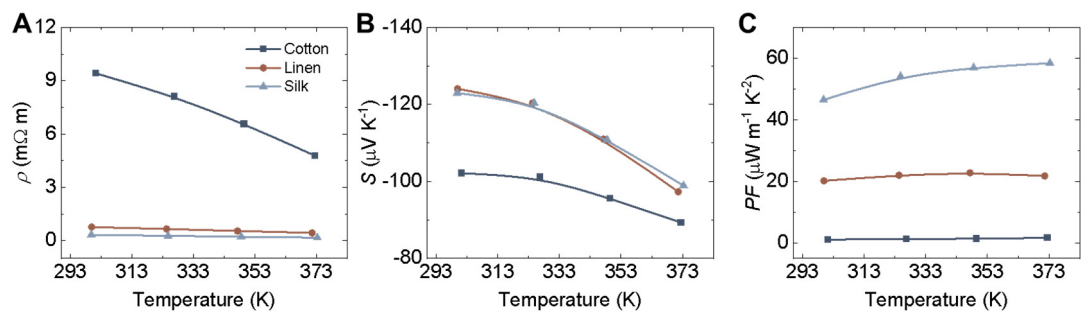


Fig. S19. Electrical resistivity (A), Seebeck coefficient (B) and power factor (C) of the thermoelectric textile.

Table S1. The element ratio in prepared Ag₂Se network.

Element	Wt%	Atomic%
Se	26.07	32.51
Ag	73.93	67.49
Total:	100.00	100.00

Table S2. The simulation conditions and parameters.

Parameters	Values	Source
Thermal conductivity of Ag ₂ Se network	0.04 W m ⁻¹ K ⁻¹	Measurement
Thermal conductivity of TE bulk (commercial)	1.6 W m ⁻¹ K ⁻¹	Ref. ¹
Thermal conductivity of copper	400 W m ⁻¹ K ⁻¹	COMSOL
Thermal conductivity of filler (PDMS)	0.15 W m ⁻¹ K ⁻¹	Ref. ^{2,3}
Resistivity of Ag ₂ Se network	1.16 × 10 ⁻³ Ω m	Measurement
Resistivity of TE bulk (commercial)	9.9 × 10 ⁻⁶ Ω m	Ref. ¹
Resistivity of copper	1.7 × 10 ⁻⁸ Ω m	COMSOL
Seebeck coefficient of Ag ₂ Se network	-130 μV K ⁻¹	Measurement
Seebeck coefficient of TE bulk (commercial)	-197 μV K ⁻¹	Ref. ¹
Heat transfer coefficient of skin surface	39.2 W m ⁻² K ⁻¹	Ref. ^{3,4}
Heat transfer coefficient of air	10.5 W m ⁻² K ⁻¹	Ref. ⁴
Skin surface temperature	306 K	Ref. ^{3,4}
Module height (full filled / 10% filled / networked)	3 mm	–
Fill factor (full filled / 10% filled / networked)	100% / 10% / 100%	–

References

- 1 Liu, Y. *et al.* Passive Radiative Cooling Enables Improved Performance in Wearable Thermoelectric Generators. *Small* **18**, e2106875 (2022).
- 2 Suarez, F. *et al.* Flexible Thermoelectric Generator Using Bulk Legs and Liquid Metal Interconnects for Wearable Electronics. *Appl. Energy* **202**, 736-745 (2017).
- 3 Ozturk *et al.* Designing Thermoelectric Generators for Self-Powered Wearable Electronics. *Energy Environ. Sci.* (2016).
- 4 Kim, C. S. *et al.* Structural Design of a Flexible Thermoelectric Power Generator for Wearable Applications. *Appl. Energy* **214**, 131-138 (2018).